Multi-objective Automatic Design of Permanent Magnet Motor Using Monte Carlo Tree Search

Hayaho Sato[1] and Hajime Igarashi[1]

[1]Graduate School of Information Science and Technology, Hokkaido University, Hokkaido 060-0814, Japan

This study proposes a novel multi-objective design method based on Monte Carlo tree search (MCTS) for the design of permanent magnet motors. The global configurations that define the entire structure are represented by nodes in a tree structure. After MCTS is performed to select a route extending from the root to leaf node, multi-objective topology optimization (TO) is performed at the leaf node to determine the detailed shape, considering a trade-off relationship among objective functions. The novelty of this work lies in the integration of MCTS with multi-objective TO where the score of a node is provided by the number of Pareto solutions obtained by selecting that node. This enables the scoring of nodes and the determination of the node selection criterion. The proposed method is applied to the multi-objective optimization of a permanent magnet motor with respect to average torque, and either torque ripple or iron loss. The proposed method successfully obtained Pareto solutions, which comprise various global configurations and shapes.

Index Terms— **Design optimization, permanent magnet (PM) motors, tree data structures.**

I. Introduction

THE OPTIMAL DESIGN of electric machines is becoming increasingly crucial owing to the realization of high-efficiency machines. Among them, permanent magnet (PM) motors are particularly significant for use in electric vehicles. To design the shape of PM motors, topology optimization (TO), where a novel shape can be found by freely deforming its magnetic core, is a promising option for performance enhancement [1], [2]. However, the performance of PM motors cannot be determined by their shapes alone but depends on the number of poles, type of PMs, and other "global" configurations, which define the entire structure. Shape optimization methods, including TO, cannot achieve optimization of the global configurations in conjunction with the shape.

Automatic design methods based on tree search have proven effective in resolving the aforementioned problem [3], [4]. In the tree search, a route extending from the root to leaf nodes is selected. This procedure corresponds to the selection of possible combinations of global configurations. Shape optimization is performed at the leaf node to determine the optimal shape under the selected global configurations. By repeating this process, the optimal combination of global configurations and detailed machine shapes can be determined. However, the algorithm was designed only for single-objective problems. The Pareto solutions cannot be obtained by running multiple single-objective optimizations for non-convex functions. For this reason, extension of the tree search to multi-objective problems has been required.

This study proposes a novel automatic design method to realize multi-objective optimization considering global configurations in conjunction with the machine shape. In this method, Monte Carlo tree search (MCTS) [5], [6] is adopted as the tree search method. During the proposed optimization, the number of Pareto solutions is considered a criterion of the score of each node in the tree. This allows for the effective integration of multi-objective shape optimization and MCTS. This method applies to the optimization of a PM motor for electric vehicles where average torque and either torque ripple or iron loss are considered simultaneously.

Manuscript received April 1, 2015; revised May 15, 2015 and June 1, 2015; accepted July 1, 2015. Date of publication July 10, 2015; date of current version July 31, 2015. Corresponding author: Hayaho Sato (e-mail: hayaho_sato@em.ist.hokudai.ac.jp).

Color versions of one or more of the figures in this paper are available online at http://ieeexplore.ieee.org.

Digital Object Identifier (inserted by IEEE).

II. Multi-objective Automatic Design Method

A. Optimization Problem for Automatic Design

First, we define the optimization problem for the automatic design as follows.

$$\min. F_k(\boldsymbol{s}, \boldsymbol{r}) \ (k = 1, \ldots, n_\mathrm{f}), \tag{1a}$$

$$\text{sub. to } G_l(\boldsymbol{s}, \boldsymbol{r}) \geq 0 \ \left(l = 1, \ldots, n_\mathrm{g}\right), \tag{1b}$$

where F_k represent the objective functions and G_l represents constraints. In the automatic design, the design variables consist of global configurations $\boldsymbol{s}$ and shape parameters $\boldsymbol{r}$. Our objective is to simultaneously optimize $\boldsymbol{s}$ and $\boldsymbol{r}$ to obtain solutions with a trade-off relationship among F_k under constraints G_i. Hereinafter, a two-objective problem ($n_\mathrm{f} = 2$) is assumed for simplicity. The proposed method can be directly extended to more than three objectives.

B. Automatic Design Using Monte Carlo Tree Search

The proposed method is shown in Fig. 1. This study considers the following global configurations: number of poles P_n, input current phase angle (current advance angle) β, type of PMs (I, V, U, ∇), and number of PMs [4]. Each level of the tree corresponds to a global configuration, and each node in the level represents a possible option. For example, we set $P_\mathrm{n} = \{4, 6, 8\}$ as possible options, such that the first level of the tree has three nodes. Each node i stores the number of visits n_i and the score v_i, indicating its optimality for the objectives, which is discussed in detail in section II. C.

The following is the algorithm of MCTS for the automatic design:

1. Set $n_i \leftarrow 0$ and $v_i \leftarrow 0$ for all nodes. Set iteration count

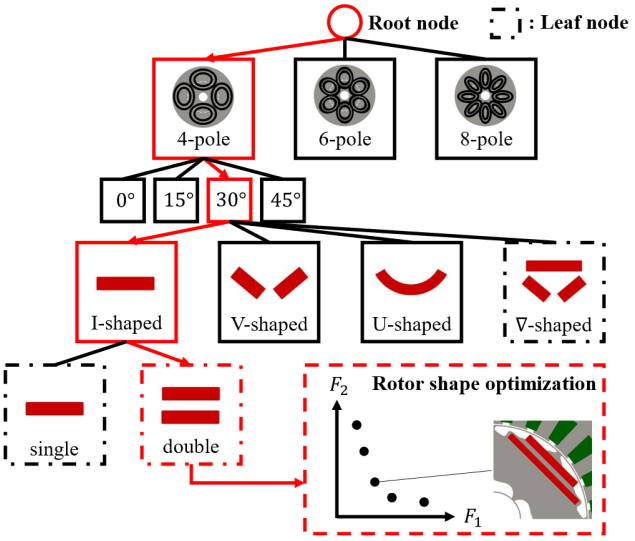

Fig. 1. Overview of the proposed method for automatic design. The layers correspond to the number of poles, input current phase angle, type of PMs, and number of PMs. The minimization problem is assumed in rotor shape optimization.

$t \leftarrow 0$.

2. Set the root node as the current node p.
3. *Selection*: Select a child node under the current node p. Node i with the maximum value of $P(p,i)$ among the children is selected [5]:

$$P(p,i) = v_i + C\sqrt{\frac{\ln n_p}{n_i}}, \tag{2}$$

where C is the constant that controls the balance between exploitation and exploration, set to 3.0 in this study to obtain diverse solutions. If n_i is zero, $P(p,i)$ is set to a large constant value. Move the current node $p \leftarrow i$.

4. If a leaf node is reached, go to step 5. Otherwise, return to step 3.
5. *Optimization*: Perform multi-objective TO to determine the rotor shape $\boldsymbol{r}$ under the selected $\boldsymbol{s}$. We adopt the NGnet on/off method [1], [2] for TO of the rotor core shown in Fig. 2. In this method, the material in position $\boldsymbol{x}$ is determined from the sign of the shape function

$$y(\boldsymbol{x},\boldsymbol{w}) = \sum_{i=1}^{N_G} w_i b_i(\boldsymbol{x}), \tag{3}$$

where $b_i(\boldsymbol{x})$ is the normalized Gaussian basis function that is uniformly placed in the rotor region. The material is set to magnetic core in the region where $y \geq 0$ holds, otherwise it is set to air. Here, the weight $\boldsymbol{w}$ is optimized to obtain the optimal shape of the rotor. Moreover, the positions and shapes of PMs are represented by parameters $\boldsymbol{p}$ (shown in Fig. 3) such that the total shape variable is $\boldsymbol{r} = \{\boldsymbol{w}, \boldsymbol{p}\}$ [2]. We obtain Pareto solutions $(\boldsymbol{s}, \boldsymbol{r}_1), (\boldsymbol{s}, \boldsymbol{r}_2), \ldots$ which are stored in the selected leaf node.
6. *Backpropagation*: Backpropagate the Pareto solutions and update v_i for the selected nodes. This process is explained in detail in Section II. C. Set $n_i \leftarrow n_i + 1$ for the selected nodes.

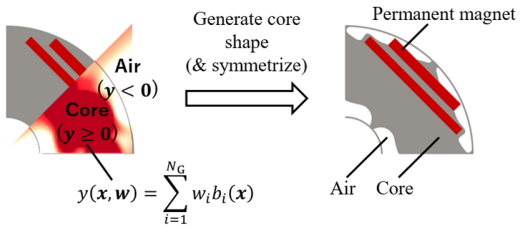

Fig. 2. NGnet on/off method.

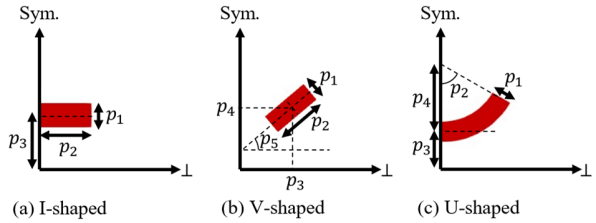

Fig. 3. Shape parameters for PMs. "Sym." and "⊥" denotes the symmetrical and perpendicular axes of motors, respectively. ∇-shaped PMs are represented by combining I- and V-shaped PMs.

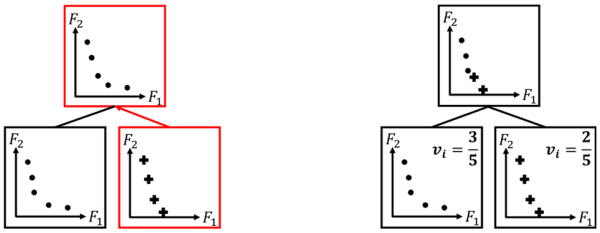

Fig. 4. MCTS backpropagation process.

7. If t reaches a given number, $t_{\max}$, terminate the process and sort the obtained Pareto solutions. Otherwise, set $t \leftarrow t + 1$ and return to step 2.

By repeating the aforementioned process, Pareto solutions under different $\boldsymbol{s}$ are gradually stored in the tree. Finally, a set of solutions with a trade-off relationship, considering the optimality of $\boldsymbol{s}$ can be determined. Moreover, selection strategy (2) enables the effective exploration of tree nodes by considering the score v_i.

C. Scoring Criterion for Monte Carlo Tree Search

MCTS requires v_i to calculate the selection strategy (2). A criterion to score multi-objective optimization results is the area of the region enclosed by the Pareto solution [6]. However, obtaining a desirable Pareto front in the automatic design using this scoring method is challenging because simple increase in the area tends to lead to solutions biased in one direction whereas such solutions would not be worthy for design of electric motors.

In the proposed method, we evaluate v_i using the number of Pareto solutions. The backpropagation process of our MCTS is shown in Fig. 4. When Pareto solutions are backpropagated from a leaf node to parent nodes, they are combined and sorted in the parent node, such that solutions in the parent node are a mixture of solutions from children nodes. Thus, we evaluate v_i for a child node i as follows.

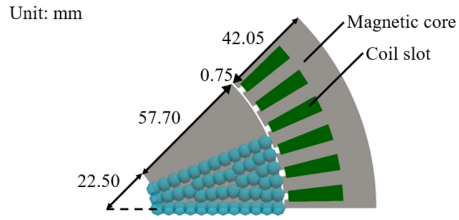

Fig. 5. Motor model for optimization. The circles represent Gaussian basis functions. The stator radius is adjusted for each P_n.

$$v_i \leftarrow \frac{N_\mathrm{P}(i,p)}{\sum_{j=1}^{N_\mathrm{c}(p)} N_\mathrm{P}(j,p)}, \tag{4}$$

where $N_\mathrm{c}(p)$ is the number of children of the parent node p, and $N_\mathrm{P}(j,p)$ is the number of Pareto solutions of child node j,which are also stored as Pareto solutions in the parent node. In other words, v_i is the normalized number of Pareto solutions of the child node, valid even in the parent node. This enables us to effectively integrate multi-objective TO and MCTS. In step 6 of the algorithm, this calculation is recursively performed until the root node is reached.

III. Numerical Results

This section presents the numerical results. We considered two trade-off problems of the PM motor: average torque vs. torque ripple, and average torque vs. iron loss. First, we present the optimization settings, followed by the numerical results of each problem.

A. Optimization Settings

We consider the PM motor shown in Fig. 5 for electric vehicles with $P_\mathrm{n} = 8$ [7]. The motor model with the other P_n has the same settings. We adopted NSGA-II for the multi-objective TO [8]. The motor and NSGA-II parameters are listed in Table I. In TO, we imposed common constraints for each problem, which are:

$$G_1(\boldsymbol{s},\boldsymbol{r}) = 3.18\times10^{-3} - S \geq 0, \tag{5a}$$

$$G_2(\boldsymbol{s},\boldsymbol{r}) = 0.10S - S_\mathrm{demag} \geq 0, \tag{5b}$$

$$G_3(\boldsymbol{s},\boldsymbol{r}) = \min\left(\frac{S_1}{S_2},\frac{S_2}{S_1}\right) - 0.75 \geq 0, \tag{5c}$$

$$G_4(\boldsymbol{s},\boldsymbol{r}) = 1 - N_\mathrm{r} \geq 0. \tag{5d}$$

The meanings of the constraints are as follows: G_1 restricts the area of PM S to be less than $3.18\times10^{-3}\mathrm{m}^2$. G_2 restricts the area of the demagnetized PM S_demag to be less than 10% of the total area, to prevent performance degradation. G_3 is imposed only when the number of PMs is two or the type of PMs is ∇, to maintain the ratio of two PMs and prevent convergence to a single PM [9]. Finally, G_4 imposes the connectivity of the magnetic core; the number of the cores, N_r, has to be one. They are evaluated by finite element method and constraint NSGA-II [8] is adopted to impose them during optimization.

B. Case I: Average Torque vs. Torque Ripple

In the first problem, our objectives were to maximize the average torque T_avg and to minimize the torque ripple T_rip. We defined the problem as follows:

$$\min. F_1(\boldsymbol{s},\boldsymbol{r}) = -T_\mathrm{avg}, \tag{6a}$$

$$\min. F_2(\boldsymbol{s},\boldsymbol{r}) = T_\mathrm{rip}. \tag{6b}$$

The Pareto solutions after 30 iterations ($t_\mathrm{max} = 30$) are shown in Fig. 6. Notably, the Pareto solutions comprise different sets of $\boldsymbol{s}$ and $\boldsymbol{r}$. For comparison, we also plotted solutions obtained by performing TO 30 times under random configurations $\boldsymbol{s}$. Using the proposed method, Pareto solutions with different $\boldsymbol{s}$ are successfully obtained. In the range where $T_\mathrm{avg} \leq 260$ Nm, the proposed method is superior over random TO. However, we found better solutions by random TO where $T_\mathrm{avg} > 260$Nm. This would result from stochastic property in MCTS and NSGA-II. Note that random TO relies on finding of good Pareto solutions by chance while MCTS systematically searches for them. Moreover, the Pareto solutions comprise motors with $P_\mathrm{n} = 8$. This suggests that 8-pole motors have better torque characteristics compared with the other number of poles.

The optimized motor shapes of typical Pareto solutions are shown in Fig. 7. Double U-shaped PMs have a higher average torque. The single I-shaped PM reduces the torque ripple and average torque. The single V-shaped PM has a good balance. The type of PMs have considerable effect on torque characteristics and should be selected properly in the design of PM motors.

TABLE I
Analysis and Optimization Parameters

Parameter	Value
Number of coil slots per pole	6
Magnetic core sheet	50A400
Thickness (mm)	50.0
Current amplitude (A)	240.4
Number of coil turns (turns)	*
Rotation speed (rpm)	1800
Residual flux density (T)	1.25
Number of Gaussian basis functions, N_G	50
Size of the group in NSGA-II	300
Crossover method in NSGA-II	SBX
Number of children in NSGA-II	150
Number of generations in NSGA-II	400

*Number of coil turns for $P_\mathrm{n} = 8$ is ten. For the other P_n, it is set to realize the same input current density as $P_\mathrm{n} = 8$.

C. Case II: Average Torque vs. Iron Loss

In the second problem, our objectives changed to maximizing the average torque T_avg and minimizing iron loss P_iron, which are defined as follows.

$$\min. F_1(\boldsymbol{s},\boldsymbol{r}) = -T_\mathrm{avg}, \tag{7a}$$

$$\min. F_2(\boldsymbol{s},\boldsymbol{r}) = P_\mathrm{iron}. \tag{7b}$$

The Pareto solutions after 30 iterations ($t_\mathrm{max} = 30$) are shown in Fig. 8. PM motors with $P_\mathrm{n} = 6, 8$ could not be the Pareto solutions. This is because the frequency is proportional to P_n at fixed rotational speed, and thus P_iron increases with P_n.

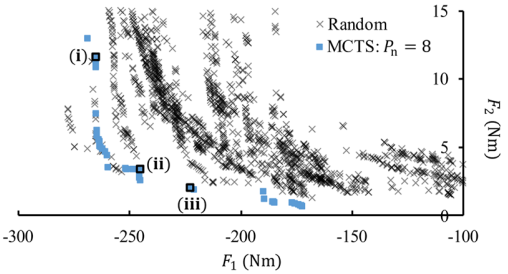

Fig. 6. Pareto solutions in optimization case I. Approximately three days were consumed to finish 30 iterations of proposed method with Intel(R) Xeon(R) Platinum 8280 x 4 (clock frequency: 2.7GHz, 112 cores, 224 threads in total).

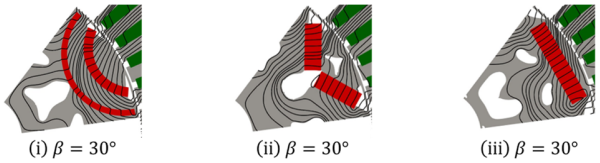

Fig. 7. Rotor shapes of Pareto solutions in optimization case I. Current phase angle β is shown below each motor. Black lines represent flux lines.

This result suggests that the proposed method can determine suitable global configurations according to the optimization problems. Moreover, the Pareto solutions obtained using the proposed method overlaps in part with the best solutions of the random TO while the former obtains the Pareto solutions not obtained by the latter.

The optimized motor shapes are shown in Fig. 9. In the region in which P_{iron} is small, the ∇-shaped PM is placed in the rotor with large flux barriers. This effectively reduces P_{iron}, whereas T_{avg} is also small. The double I-shaped PM can enhance T_{avg} with a considerable P_{iron}. In this case, Pareto solutions tend to have double-layered PMs with $\beta = 45°$. This might be because they enhance the reluctance torque and suppress P_{iron} that originates from the magnet-derived torque.

It is not difficult to extend the proposed method to problems with more than three objectives. Fig. 10 shows Pareto solutions to a three-objective problem with respect to $-T_{\mathrm{avg}}$, T_{rip} and S obtained by the proposed method. The three-dimensional Pareto solution is obtained after 25 iterations.

IV. Conclusion

This study proposed a novel multi-objective automatic design method based on MCTS and multi-objective TO. The proposed method could effectively design PM motors by considering global configurations and detailed rotor shapes. The constructed tree can be used for other optimization problems. Moreover, we can extract useful knowledge from the resultant tree after optimization which contains the nodal scores.

Acknowledgment

This study was supported by JST SPRING, Grant Number JPMJSP2119, the MEXT Doctoral program for Data-Related InnoVation Expert Hokkaido University (D-DRIVE-HU) program, and KAKENHI 21H01301.

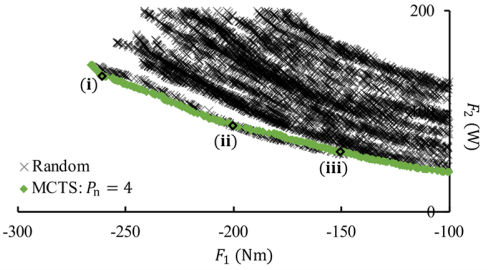

Fig. 8. Pareto solutions in optimization case II. Approximately five days were consumed to finish 30 iterations of proposed method with Intel(R) Xeon(R) Platinum 8280 x 4 (clock frequency: 2.7GHz, 112 cores, 224 threads in total).

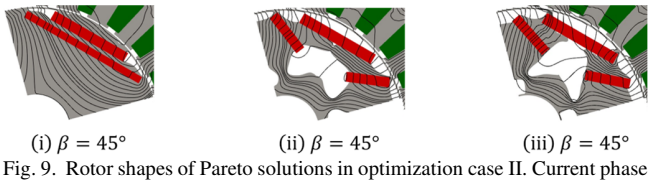

Fig. 9. Rotor shapes of Pareto solutions in optimization case II. Current phase angle β is shown below each motor. Black lines represent flux lines.

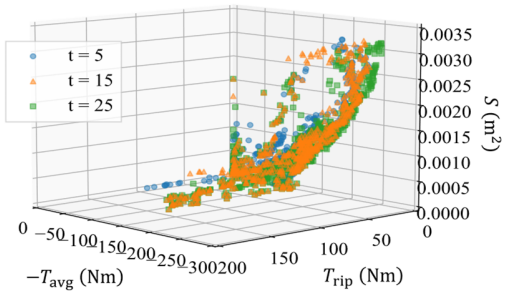

Fig. 10. Pareto solutions to three-objective problem with respect to $-T_{\mathrm{avg}}$, T_{rip} and S at iteration counts $t = 5, 15,$ and 25.

References

[1] T. Sato, K. Watanabe, and H. Igarashi, "Multimaterial Topology Optimization of Electric Machines Based on Normalized Gaussian Network," *IEEE Trans. Magn.*, vol. 51, no. 3, Art no. 7202604, 2015.

[2] S. Hiruma, M. Ohtani, S. Soma, Y. Kubota, and H. Igarashi, "Novel Hybridization of Parameter and Topology Optimizations: Application to Permanent Magnet Motor," *IEEE Trans. Magn.,* vol. 57, no. 7, Art no. 8204604, 2021.

[3] T. Sato and M. Fujita, "A Data-Driven Automatic Design Method for Electric Machines Based on Reinforcement Learning and Evolutionary Optimization," *IEEE Access*, vol. 9, pp. 71284–71294, 2021.

[4] H. Sato and H. Igarashi, "Automatic Design of PM Motor Using Monte Carlo Tree Search in Conjunction with Topology Optimization," *IEEE Trans. Magn.*, vol. 58, no. 9, Art no. 7200504, 2022.

[5] Guillaume M.J-B. Chaslot, Mark H.M. Winands, H. Jaap Van Den Herik, and Jos W.H.M. Uiterwijk, "Progressive Strategies for Monte-Carlo Tree Search," *New Math. And Nat.*, vol. 4, no. 3, pp. 343–357, 2008.

[6] W. Wang and M. Sebag, "Multi-objective Monte-Carlo Tree Search", *Proc. the Asian Conference on ML*, vol. 25, pp. 507–522, 2012.

[7] T.A. Burres, S.L. Campbell, C.L. Coomer, C.W. Ayers, A.A. Wereszczak, J.P. Cunningham, L.D. Marlino, L.E. Seier, and H.T. Lin, "Evaluation of the 2010 TOYOTA PRIUS Hybrid Synergy Drive System," ORNL/TM-2010/253, Oak Ridge National Laboratory, Oak Ridge, Tennessee, 2011.

[8] K. Deb, A. Pratap, and S. Agarwal, "A fast and elitist multiobjective genetic algorithm: NSGA-II," *IEEE Trans. Evol. Comput.,* vol. 6, no. 2, pp. 115–148, 2002.

[9] Y. Otomo, T. Abe, H. Igarashi, T. Kato, and H. Kurita, "Optimization of permanent magnet configuration using Boolean geometry projection method for IPM motors," *CEFC2022*, P03, 2022.